Articles

Controlling the Melting of Kinetically Frozen Poly(butyl acrylate-*b*-acrylic acid) Micelles via Addition of Surfactant

Marc Jacquin,[†] Pierre Muller,[†,‡] Hervé Cottet,[§] Regan Crooks,[||] and Olivier Théodoly*,[†,⊥]

Complex Fluids Laboratory, CNRS UMR 166, and Bristol Research & Technology Center, Rhodia, 350 George Patterson Boulevard, Bristol, Pennsylvania 19007, Equipe Dynamique des Systèmes Biomoléculaires Complexes, CNRS UMR 5073, Université de Montpellier 2, place Eugène Bataillon CC 017, 34095 Montpellier Cedex 5, France, Institut Charles Sadron, CNRS UPR 22, 6 rue Boussingault, 67083 Strasbourg Cedex, France, Laboratoire Adhésion et Inflammation, INSERM U600, CNRS UMR 6212, Case 937, 163 Avenue de Luminy, Marseille F-13009, France, and Faculté des Sciences/de Médecine ou de Pharmacie, Aix-Marseille Université, Marseille F-13000, France

Received February 8, 2007. In Final Form: May 14, 2007

We have studied the melting of polymeric amphiphilic micelles induced by small-molecule surfactant and explained the results by experimental determination of the interfacial tension between the core of the micelles and the surfactant solutions. Poly(*n*-butyl acrylate-*b*-acrylic acid) (PBA-*b*-PAA) amphiphilic diblock copolymers form kinetically frozen micelles in aqueous solutions. Strong interactions with surfactants, either neutral or anionic [C12E6, C6E4, sodium dodecyl sulfate (SDS)], were revealed by critical micelle concentration (cmc) shifts in specific electrode and surface tension measurements. Since both polymer and surfactant are either neutral or bear negative charges, the attractive interactions are not due to electrostatic interactions. Light scattering, neutron scattering, and capillary electrophoresis experiments showed important structural changes in mixed PBA-*b*-PAA/surfactant systems. Kinetically frozen micelles of PBA-*b*-PAA, that are hardly perturbed by concentration, ionization, ionic strength, and temperature stresses, can be disintegrated by addition of small-molecule surfactants. The interfacial energy of the PBA in surfactant solutions was measured by drop shape analysis with h-PBA homopolymer drops immersed in small-molecule surfactant solutions. The PBA/water interfacial energy $\gamma_{\mathrm{PBA/H_2O}}$ of 20 mN/m induces a high energy cost for the extraction of unimers from micelles so that PBA-*b*-PAA micelles are kinetically frozen. Small-molecule surfactants can reduce the interfacial energy $\gamma_{\mathrm{PBA/solution}}$ to 5 mN/m. This induces a shift of the micelle−unimer equilibrium toward unimers and leads, in some cases, to the apparent disintegration of PBA-*b*-PAA micelles. Before total disintegration, polymer/surfactant mixtures are dispersions of polydisperse mixed micelles. Based on core interfacial energy arguments, the disintegration of kinetically frozen polymeric micelles was interpreted by gradual fractionation of objects (polydisperse dispersion mechanism), whereas the disintegration of polymeric micelles in a thermodynamically stable state was interpreted by an exchange between a population of large polymer-rich micelles and a population of small surfactant-rich micelles (bidisperse dispersion mechanism). Finally, in our system and other systems from the literature, interfacial energy arguments could explain why the disintegration of polymer micelles is either partial or total as a function of the surfactant type and concentration and the hydrophobic block molar mass of the polymer.

1. Introduction

Water-soluble surface-active block copolymers have great potential as additives to common small-molecule surfactant formulations. In what follows, for the sake of simplicity, we call "amphiphilic diblocks" all amphiphilic molecules whose mass is in the range 5000−30 000 Da and "surfactant" all small amphiphilic molecules whose mass is in the range 100−500 Da. Typical applications of amphiphilic diblocks enclose formulations based on surfactants, designed for detergency, suspension stabilization, emulsion polymerization, or wetting modification. One target of polymeric surfactant additives may be to improve already well-performing formulations in order to increase their efficiency[1] or to decrease their production cost. For instance, some emulsion polymerization processes use surfactants that are poor stabilizers of the emulsion but good catalysts for the polymerization. Addition of a small quantity of amphiphilic diblock copolymers can improve the stabilization characteristics and keep the catalytic effect at the same time.[2,3] Other applications take advantage of the self-assembling properties of surfactants and block copolymers, which form micelles in solution of typical diameter 2−10 nm for surfactant and 10−200 nm for block copolymers. Mixtures of both often lead to the formation of mixed micelles that can be used as templates for nanoparticle formation[4] or could be used for controlled drug delivery.[5,6] The

---

* Corresponding author: tel +33 (0)4 91 82 75 79; fax +33 (0)4 91 82 75 80; e-mail: theodoly@marseille.inserm.fr.

[†] Complex Fluids Laboratory, Rhodia.

[‡] Institut Charles Sadron.

[§] Université de Montpellier 2.

[||] Bristol Reseach & Technical Center, Rhodia.

[⊥] Laboratoire Adhésion et Inflammation and Aix-Marseille Université.

(1) Deroo, S.; Morvan, M. World Patent WO 03068848, 2003.

(2) Herve, A.; Liu, W.- L. U.S. Patent 6,825,290 and EU Patent EP1419181, 2004.

(3) Herve, A.; Joanicot, M.; Kiplinger, J. D.; Morvan, M. U.S. Patent 7,105,579, 2006.

(4) Bronstein, L. M.; Chernyshow, D. M.; Timofeeva, G. I.; Dubrovina, L. V.; Valetsky, P. M.; Obolonkova, E. S.; Khokhlov, A. R. *Langmuir* **2000**, *16*, 3626−3632.

(5) Rösler, A.; Vandermeulen, G. W. M.; Klok, H. A. *Adv. Drug Delivery Rev.* **2001**, *53*, 95−108.

10.1021/la700370f CCC: $37.00

behavior of diblock copolymers in the presence of surfactants is therefore of great importance to control the properties of mixtures. Strong coupling of diblock copolymers and surfactants lead to new specific properties, both in solutions and at interfaces.

Homopolymer–surfactant interactions in dilute aqueous solutions have been extensively studied in the literature.[7–9] Concerning block copolymers, much attention has been devoted to the complexation of oppositely charged polymers and surfactants. These systems are characterized by very strong attractive electrostatic interactions, which lead to the formation of flocks and/or coacervates.[10–13] In this work, we consider mixtures of amphiphilic diblock copolymers and surfactants with no attractive electrostatic interactions. Polymers and surfactants are either neutral or bearing same sign charges. The main interactions are therefore of hydrophobic origin, that is, association driven by the minimization of interfacial energies in solutions. Although this problem has recently attracted much attention,[14–30] the understanding of these systems is far from complete. The first reason is that the various chemistries studied in the literature lead to several types of behavior, so that no universal picture of the phenomenon has emerged. For instance, polymer samples themselves have very different properties: some are at equilibrium in solution, like the poly(ethylene oxide-*b*-propylene oxide) PEO-*b*-PPO Pluronics,[14–21] whereas others are clearly out of equilibrium, like poly(styrene-*b*-ethylene oxide) PS_{10}-*b*-PEO_{68},[28] poly(styrene-*b*-sodium methacrylate) PS_{28}-PMA_{87} or poly(*tert*-butylstyrene-*b*-sodium methacrylate) $PtBS_{27}$-PMA_{70}.[27] Nevertheless, among all these results and systems, some trends appear to be clear. For the Pluronics family, all observations converge to a picture of complete disintegration of polymeric micelles upon addition of surfactant. Complete disintegration is also observed in other cases like poly(oxyphenylethylene-*b*-ethylene oxide) $POPE_{17}PEO_{65}$ with SDS[29] and SeDS[30] and poly(butadiene-*b*-ethylene oxide) PB_{45}-PEO_{126} with $C_{12}E_5$.[24] In all other systems, some disintegration is observed but this disintegration is not complete. There is no consensus to explain why the disintegration is only partial in certain cases. The explanations that have been proposed include a triblock effect,[24] a packing effect,[26] and a surfactant effect.[30] In the latter case, the authors observed, with the same polymer, either a complete or a partial disintegration depending on the nature of the surfactant added. Also, in all systems, the path toward disintegration is not clearly understood. One reason is the difficulty of obtaining very precise data on size distributions by dynamic light scattering (DLS). Depending on the system or the solvent conditions, some authors observe a single population of micelles whose mean diameter decreases continuously.[20,21] Others report a double population of small surfactant-rich mixed micelles and large polymer-rich mixed micelles during the disintegration process ("peeling off mechanism").[20,21,24,29,30] Again, no mechanistic explanation is proposed to explain how these processes take place.

In this work, we have tried to investigate the different parameters that may influence the interactions between a diblock polymer and a surfactant and attempted to clarify the physics at stake for the complexation and disintegration processes. We have paid a special attention to the role of reversibility of the complexation and to the key role of interfacial tension between the core of micelles and the solution. We have used diblock copolymers of poly(butyl acrylate-*b*-acrylic acid), PBA-*b*-PAA. On one hand, it is again another chemistry, whose behavior with surfactants has never been studied. However, these samples that we synthesized ourselves have allowed us to tune many parameters concerning the polymer. Depending on pH, PBA-*b*-PAA can be either neutral or charged, whereas all structural studies of diblocks and surfactant mixtures in the literature concern neutral diblocks. Also, by use of PBA-*b*-PAA samples with different ratios between PBA and PAA, that is, tuning the hydrophilic–lypophilic balance of the samples, we can start from cylindrical or spherical micelles, which was also a parameter claimed to be of importance in the literature. Also, we have been able to study a series of polymers with different block lengths but the same PBA/PAA mass ratio, which affects the theoretical exchange kinetics of unimers between their state in micelles and in solution. This exchange kinetics is rarely discussed in other systems in the literature, even though it strongly differs from one system to the other: The diblock copolymers PBA-*b*-PAA considered here form micellar dispersions in water that are irreversibly aggregated or kinetically frozen.[31] For what concerns the surfactant parameters, we have chosen samples with different charges and critical micelle concentration (cmc) values (see Table 2). This allowed us to tune the interfacial tension between the core of PBA of the polymeric micelles and the surfactant solution by changing the concentration and the nature of the surfactant. This interfacial tension has been systematically measured in order to establish a quantitative link with the state of the polymer/surfactant solutions. In the end, our physical description of the polymer/surfactant interactions permits us to explain why disintegration can be total or partial in polymer/surfactant complexation and also why different intermediate states, with single or double populations, can be observed.

---

(6) Torchilin, V. P. *J. Controlled Release* **2001**, *73*, 137–172.

(7) Goddard, E. D.; Ananthapadmanabhan, K. P. *Interactions of Surfactants with Polymers and Proteins*; CRC Press: Boca Raton, FL, 1993.

(8) Jönsson, B.; Lindman, B.; Holmberg, K.; Kronberg, B. *Surfactants and Polymers in Aqueous Solutions*; John Wiley & Sons: New York, 1999.

(9) Kwak, J. C. T. *Polymer–Surfactant Systems*; Surfactant Science Series, Vol. 77; Marcel Dekker: New York, 1998.

(10) Bronich, T. K.; Kabanov, A. V.; Kabanov, V. A.; Yu, K.; Eisenberg, A. *Macromolecules* **1997**, *30*, 3519.

(11) Bronich, T. K.; Popov, A. M.; Eisenberg, A.; Kabanov, V. A.; Kabanov, A. V. *Langmuir* **2000**, *16*, 481.

(12) Hervé, P.; Destarac, M.; Berret, J.-F.; Oberdisse, J.; I. Grillo, I. *Europhys. Lett.* **2002**, *58* (6), 912–918.

(13) Cohen Stuart, M. A.; Hofs, P. S.; Voets, I. K.; de Keizer, A. *Curr. Opin. Colloid Interface Sci.* **2005**, *10* (1–2), 30–36.

(14) Almgren, M.; van Stam, J.; Lindblad, C.; Li, P.; Stilbs, P.; Bahadur, P. *J. Phys. Chem.* **1991**, *95*, 5677–5684.

(15) Hecht, E.; Mortensen, K.; Gradzielski, M.; Hoffman, H. *J. Phys. Chem.* **1995**, *99*, 4866–4874.

(16) Hecht, E.; Hoffmann, H. *Langmuir* **1994**, *10*, 86–91.

(17) Li, Y.; Xu, R.; Couderc, S.; Bloor, D. M.; Wyn Jones, E.; Holzwarth, J. F. *Langmuir* **2001**, *17*, 183–188.

(18) Thurn, T.; Couderc, S.; Sidhu, J.; Bloor, D. M.; Penfold, J.; Holzwarth, J. F.; Wyn Jones, E. *Langmuir* **2002**, *18*, 9267–9275.

(19) Li, Y.; Xu, R.; Couderc, S.; Bloor, D. M.; Holzwarth, J. F.; Wyn Jones, E. *Langmuir* **2001**, *17*, 5742–5747.

(20) Cardoso da Silva, R.; Olofsson, G.; Schillén, K.; Loh, W. *J. Phys. Chem. B* **2002**, *106*, 1239–1246.

(21) Jansson, J.; Schillén, K.; Olofsson, G.; Cardoso da Silva, R.; Loh, W. *J. Phys. Chem. B* **2004**, *108*, 82–92.

(22) Burke, S. E.; Eisenberg, A. *Langmuir* **2001**, *17*, 8341–8347.

(23) Choucair, A.; Eisenberg, A. *Eur. Phys. J.* **2003**, *10*, 37–44.

(24) Zheng, Y.; Davis, H. T. *Langmuir* **2000**, *16*, 6453–6459.

(25) Nordskog, A.; Egger, H.; Findernegg, G. H.; Hellweg, T.; Schlaad, H.; von Berlepsch, H.; Böttcher, C. *Phys. Rev. E* **2003**, *68*, 011406-–1/14.

(26) Nordskog, A.; Fütterer, T.; von Berlepsch, H.; Böttcher, C.; Heinemann, A.; Schlaad, H.; Hellweg, T. *Phys. Chem. Chem. Phys.* **2004**, *6*, 3123–3129.

(27) Van Stam, J.; Creutz, S.; De Scryer, F. C.; Jérôme, R. *Macromolecules* **2000**, *33*, 6388–6395.

(28) Bronstein, L. M.; Chernyshov, D. M.; Vorontsov, E.; Timofeeva, G. I.; Dubroina, L. V.; Valetsky, P. M.; Kazakov, S.; Khokhlov, A. R. *J. Phys. Chem. B* **2001**, *105*, 9077–9082.

(29) Castro, E.; Taboada, P.; Mosquera, V. *J. Phys. Chem. B* **2005**, *109*, 5592–5599.

(30) Castro, E.; Taboada, P.; Barbosa, S.; Mosquera, V. *Biomacromolecules* **2005**, *6*, 1438–1447.

(31) Jacquin, M.; Muller, P.; Talingting-Pabalan, R.; Cottet, H.; Berret, J. F.; Futterer, T.; Théodoly, O. Chemical Analysis and Aqueous Solution Properties of Charged Amphiphilic Block Copolymers PBA-*b*-PAA Synthesized by MADIX. *J. Colloid Interface Sci.*, accepted for publication, http://dx.doi.org/10.1016/j.jcis.2007.08.025.

Table 1. Chemical Analysis Results for the Polymer Samples[a]

	GPC		NMR	
	M_{wBA} (g/mol)	I_{pBA}	M_{wAA} (g/mol)	$X^{\mathrm{NMR}}_{\mathrm{BA/AA}}$
PBA*-*b*-PAA 3K−12K	5430	1.5	22600	0.24
PBA*-*b*-PAA 6K−24K	6420	2.47	29200	0.22
d_9-PBA*-*b*-PAA 3K−12K				0.24
	M_{wAA} (g/mol)	I_{pAA}	M_{wBA} (g/mol)	
PBA-*b*-PAA* 1K−4K	8850	2.41	2300	0.26
PBA-*b*-PAA* 3K−4K	10 430	2.72	7200	0.69

[a] M_{wBA} and M_{wAA} are the mass-average molar masses of the blocks BA and AA, I_{p} is the index of polydispersity, and $X^{\mathrm{NMR}}_{\mathrm{BA/AA}}$ is the mass ratio of BA to AA in a sample.

2. Experimental Section

2.1. Materials: 2.1.1. Polymers. All polymers were synthesized via controlled radical polymerization process, MADIX (macromolecular design via interchange of xanthate, Rhodia Patent WO 9858974). Monomers used were *n*-butyl acrylate 99%+ (Aldrich 234923) and acrylic acid 99% (Aldrich 147230). The controlling agent was a xanthate 2-mercaptopropionic acid methyl ester *o*-ethyl dithiocarbonate (Rhodixan A1, Rhodia), and the initiator was 2,2′-azobis(2-methylbutanenitrile), AMBN (Vazo 67, DuPont). Polymerizations were performed in ethanol starting with the PBA block. The first block was grown in 40 wt % solutions at 70 °C under N_2. A shot of initiator was added to initiate the reaction with a molar ratio of initiator versus controlling agent of 0.1. After completion of the first block, a second block was grown in similar conditions (40 wt % for first block and acrylic acid in ethanol at a temperature of 70 °C under N_2) and a new shot of initiator was added to initiate the second block reaction. Time of reaction was limited to the minimum amount necessary to achieve a rate of conversion of 99%; that is, around 8 h per block. Finally, the reaction product was dialyzed versus pure water (to remove the ethanol and unreacted monomers) and freeze-dried. More details are given elsewhere.[32] Chemical analysis of polymer samples is summarized in Table 1.

2.1.2. Surfactants. Sodium dodecyl sulfate (SDS) was purchased from Ultrapure Bioreagent, J.T. Baker (purity >99.5%). Tetra(oxyethylene) hexyl ether, C6E4, was purchased from Bachem. Ultrapure hexa(oxyethylene) dodecyl ether, C12E6, was purchased from Nikko Chemical, Japan.

2.2. Techniques: 2.2.1. Capillary Electrophoresis. All experiments were based on the capillary zone electrophoresis (CZE) technique. A high voltage, typically 16 kV, was applied to a fused silica capillary filled with an electrolyte at a controlled temperature. The apparent electrophoretic mobility μ_{app} of a solute is defined according to

$$\mu_{\mathrm{app}} = \frac{v_{\mathrm{app}}}{E} = \frac{Ll}{Vt_{\mathrm{app}}} \tag{1}$$

where v_{app} is the apparent electrophoretic velocity, E is the electric field, L is the total capillary length, l is the effective capillary length, V is the applied voltage, and t_{app} is the apparent migration time of the solute. The apparent mobility differs from the effective mobility of the solute due to the electroosmotic flow. The effective mobility is determined from

$$\mu_{\mathrm{ep}} = \mu_{\mathrm{app}} - \mu_{\mathrm{eo}} = \frac{Ll}{Vt_{\mathrm{app}}} - \frac{Ll}{V_{\mathrm{eo}}} \tag{2}$$

where t_{eo} is the migration time of neutral molecules. Micellar electrokinetic chromatography (MEKC) is a particular type of CZE. In MEKC, surfactant is added in the electrolyte. The electroosmotic flow is only marginally affected when anionic or neutral surfactants are used. The effective mobility of a solute may, however, be significantly modified if this solute interacts with the surfactant. This is the case for amphiphilic diblocks, and MEKC is very helpful as a complement to nonmicellar CZE for peak identification. All CE experiments were performed on an Agilent Technologies CE capillary electrophoresis system. Capillaries were prepared from bare silica tubing purchased from Composite Metal Services (Worcester, U.K.). Capillary dimensions were $L = 33.5$ cm ($l = 25$ cm to the detector) × diameter 50 μm. The electrolyte used for the nonmicellar separations was a 160 mM sodium borate buffer at pH 9.2. For the MEKC mode, neutral surfactant (C12E6) was added to the previous electrolyte at different concentrations. The applied voltage V was +16 kV. UV detection was performed at wavelengths of 200 and 290 nm, the former being sensitive to acrylate groups and the latter being specific to xanthate. Capillaries were first conditioned with the following flushes: 1 M NaOH for 15 min and 0.1 M NaOH for 10 min. Between injections, capillaries surfaces were regenerated by the following procedure: (i) 5 min flush with 1 M NaOH, (ii) 2 min flush with 0.1 M NaOH, (iii) application of a +1 kV voltage in 0.1 M NaOH, and (iv) 5 min flush with the electrolyte. Injections of samples at 1 wt % were performed hydrodynamically with pressures between 17 and 40 mbar for 3 s. Mesityl oxide [~0.1% (v/v) in the electrolyte] was co-injected with the sample to determine the electroosmotic mobility. The temperature of the capillary cartridge was set to 25 °C.

2.2.2. Interfacial Tension. A pendant drop Rame-Hart goniometer was used to measure interfacial tensions. Air−water interfacial tensions were measured on hanging bubbles, whose volume was kept constant over time by a step-motor activated syringe controlled by a feedback loop. Liquid−liquid interfacial tensions between h-PBA and surfactant solutions have been measured on sessile drops of h-PBA immersed in water. All glassware have been cleaned in KOH-saturated ethanol solutions for 10 min and then thoroughly rinsed with MilliQ water. All solutions were prepared with Milli-Q water.

2.2.3. SDS-Specific Electrode. The SDS-selective membrane electrodes used in this work were prepared by procedures described previously.[33,34] The general concept of a surfactant-selective membrane is based on the presence of a surfactant-selective carrier. The membrane that we use here has the carrier firmly incorporated into a silica polymer membrane structure. The carrier used to assign ion selectivity to the membrane is a cetyltrimethylammonium/dodecyl sulfate (CTADS) complex, obtained by precipitation in water of stoichiometric quantities of CTAB and SDS and purification of the precipitate. To the carrier, solubilized in 1 mL of tetrahydrofuran (THF) at a concentration of 0.01 M, were added 0.4 g of copolymer PS-124 and 0.03 g of silica Aerosil 300. After complete solubilization of these compounds, 0.6 g of the reticulated polymer CAF-3 was finally added; after thorough mixing, this resulted in the formation of a thick gel that could be conserved for about 15 days when stored under argon. Membranes were formed by placing a small portion of this material as a thin layer across the orifice of a glass tube. The membranes were left for about 12 h to dry. Before use, the membranes were conditioned by exposure to an aqueous solution containing 1 mM SDS for at least 2 h. Prepared in this way, the membranes could be used repeatedly over a period of about 1 month.

2.2.4. Light Scattering. Static and dynamic light scattering experiment were performed on a Brookhaven spectrometer (BI-200S with a BI-9000AT autocorrelator). All solutions were filtered on a 0.45 μm sterile inorganic membrane filter (Whatman) before measurements. Dynamic light scattering (DLS) was used to measure the hydrodynamic radius R_{h} of micelles in solution. BI-9000AT allows acquisition of relaxation rates over 8 orders of magnitude, from 0.1 μs to 10 s, and of multiangle scans between 20° and 155°. All data were analyzed by multi-angle CONTIN analysis.

2.2.5. Small-Angle X-ray and Neutron Scattering. Small-angle neutron scattering (SANS) measurements have been performed on NG3 at National Institute of Standards and Technology (NIST),

---

[32] Jacquin, M.; Muller, P.; Bauer, C.; Lizaragua, G.; Cottet, H.; Theodoly, O. Controlled radical polymerization of PBA-*b*-PAA and PDEGA-PAA diblock copolymers by MADIX 2. *Macromolecules* **2007**, *40*, 2672−2682.

[33] Mokus, M.; Kragh-Hansen, U.; Letellier, P.; leMaire, M.; Møller, J. V. *Anal. Biochem.* **1998**, *264*, 34−40.

[34] Mokus, M. Ph.D. Thesis, University of Paris 6, Paris, France, 1996.

Gaithersburg, MD, and on PACE at Laboratoire Léon Brillouin (LLB), Saclay, France. In order to fit the data of spherical polymer micelles with highly stretched polyelectrolyte corona, we applied an urchin-like model.[35] The scattering in this model is a combination of the mean-field term for a core (radius R_c) and a stretched corona (corona profile decreases with a power law of −2) and of the term resulting from N_{agg} stretched chains of length L_{rod}. However, for our systems, as the core size is relatively large and the corona is diluted, the scattering intensity in the q-range 0.03−3 nm^{-1} is dominated by the core. This observation has already been validated by others in the literature[36] with similar contrast conditions. Consequently, adjustment of data by a form factor of polydisperse spheres gave also reasonable results. In order to fit the scattering of polymer−surfactant complex, the use of form factors of polydisperse spheres were completely justified. Indeed, as shown later in this paper, upon addition of surfactant, the mixed objects become richer and richer in surfactant compared to polymer, and the contribution of the corona becomes more and more negligible. In all treatments, we assumed a Gaussian distribution of core radii.

2.2.6. Cryo-transmission Electron Microscopy. A Jeol 1200EX-120kV instrument has been used at CRA, Rhodia, France. Solutions have been deposited on perforated carbon film grids. Excess solution was blotted off in order to form a 100 nm film in the holes of the carbon film. This preparation is immediately frozen by being dipped first in liquid ethane and after in liquid nitrogen. Ultrafast cooling is necessary to ensure vitrification of the solution and avoid artifacts due to crystallization of the solvent or reorganization of the assemblies in solution. The frozen meniscuses in the grid holes are then observed by transmission electron microscopy (TEM).

2.3. Sample Preparation: 2.3.1. Polymer Solutions. Polymer solutions were prepared by two routes. For the first route ("cast film" route), we started by preparing films of polymer melt. Solutions of 20 wt % diblock in THF (good solvent of the two blocks) were deposited in Teflon molds, allowed to evaporate slowly over 7 days, and then dried under vacuum for 3 days. Diblock chains, which were originally dispersed as unimers in THF, eventually micro-phase-separated at some stage during the solvent evaporation. It was important to ensure slow evaporation of the solvent to let the polymer organize in microstructures before it becomes solid. These micro-structured cast films were then dispersed in water. The second route ("dialysis" route) consisted of preparing a polymer solution in nonselective solvent (THF) and then exchanging the solvent by water via dialysis through a membrane of molecular weight cutoff (MWCO) 2000.

2.3.2. Polymer/Surfactant Mixtures. Most experiments were performed at a constant polymer concentration and increasing surfactant concentrations. It appeared important to avoid high local surfactant concentrations at any point during the preparation of mixtures. Addition of a concentrated surfactant to a polymer solution led to solutions with highly polydisperse objects. The chosen procedure was to dilute a small amount of a concentrated polymer solution into a solution of surfactant at the targeted concentration. The working conditions were different for the experiments in capillary electrophoresis. In this case, the surfactant is present in the mobile phase and the polymer solutions injected had no added surfactant. The time of travel in the capillary before detection is about 30 min.

3. Results and Discussion

3.1. Critical Micelle Concentration Shift. Figure 1 presents the surface tension of surfactant C12E6/polymer PBA-*b*-PAA 3K−12K aqueous solutions versus the concentration of C12E6. The curve in the absence of polymer presents a decreasing part at low concentration. By use of the Gibbs equation, the adsorbed amount of surfactant can be calculated at a maximum value of 1.14 mg/m^2, which corresponds to a saturated interface. The breakpoint at 3×10^{-3} wt % corresponds to the cmc of the pure surfactant. In a benchmark experiment, not reported in Figure 1, it was checked that the presence of homopolymer PAA at 1 wt % with a pH adjusted to 9 did not affect the surface tension value of the pure surfactant system. A series of experiments were then performed in the presence of diblock. With PBA-*b*-PAA 3K−12K, one can notice in Figure 1 that the surface tension at very low surfactant concentration is not 72 mN/m, as expected for a pure air/water interface, but rather around 57 mN/m. Indeed, PBA-*b*-PAA 3K−12K is surface-active itself. The starting surface tension at equilibrium, or in fact after 24 h of equilibration, is around 55 mN/m for a pure polymer solution. The polymer concentrations used here are well above the polymer cmc,[31] so that without any C12E6 present, the surface is saturated by polymer. With increasing C12E6 concentration, the surface tension decreases monotonically until it reaches a break point and a plateau. This plateau value is equal to the one reached in the pure surfactant system, which is a hint that the plateau corresponds to a surface that is mainly covered with surfactant. However, the concentration at the break point is very different in the mixed polymer/surfactant system from its pure surfactant system value. Also, this break-point concentration increases with the amount of polymer. It is obvious that the break point corresponds to the appearance of C12E6 micelles in the bulk solution. The fact that more C12E6 is needed to form the first pure surfactant micelles in the presence of polymer means that a fraction of C12E6 is strongly interacting with the polymer and is therefore not available for the equilibrium between surfactant micelles and free surfactant molecules. We checked that the apparent cmc increases linearly with the amount of polymer, which is consistent with the existence of strong complexation between the polymer and the surfactant. In Figure 1, we do not detect any critical aggregation concentration (cac). In fact, a cac is generally detected by surface tension measurements when (i) the polymer is not surface-active and (ii) the polymer−surfactant complex is synergistically more surface-active than the polymer or the surfactant alone;[37] that is, typically when several surfactant molecules are linked by a polymer chain. Here, the polymer is surface-active by itself. A complex between surfactant and polymer—for instance, several molecules surrounding the hydrophobic block of the polymer chain—is more soluble than the diblock chain itself and hence less surface-active. Surface tension measurement is therefore not an adequate technique to detect cac with this system. From the cmc shifts, the amount of C12E6 interacting with the polymer at saturation can be directly

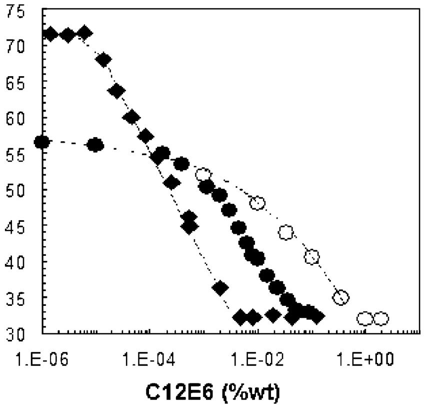

Figure 1. Surface tension versus concentration of added surfactant C12E6: (◆) without polymer in solution, in the presence of of PBA-*b*-PAA 3K−12K at ionization α = 1 and concentration (●) 0.1 and (○) 1.5 wt %.

---

[35] Muller, F.; Delsanti, L.; Auvray, L.; Guenoun P.; Yang, J.; Chen, Y. J.; Mays, J. W.; Démé, B.; Tirrell, M.; Guenoun, P. *Eur. Phys. J. E* **2000**, *3*, 45−53.

[36] Plĕstil, J. *J. Appl. Crystallogr.* **2000**, *33*, 600−604.

[37] Goddard, E. D. *Colloids Surf.* **1986**, *19*, 255−329.

Table 2. Characteristics of Surfactant Samples[a]

	M (g/mol)	cmc (wt %)	A_0 (Å^2)
C12E6	450.66	3×10^{-3}	110 ± 5
C6E4	278.37	3	80 ± 5
SDS	288.38	0.2	100 ± 5

[a] *M* is the molar mass, cmc is the critical micelle concentration in water, and A_0 is the area per molecule at the air/water interface at saturation.

calculated by subtracting the apparent cmc in the presence of polymer and the cmc of the pure surfactant. We find that an average of 15 molecules of surfactant interact per molecule of polymer. But at this point, the structure of the complex is not obvious. From previous work, we know that PBA-*b*-PAA diblocks form highly stable micelles in solution with extremely low cmc values ($<10^{-4}$ wt %). The amount of free unimers in solution is negligible. If it is assumed that all the surfactant interacts with indestructible micelles, and hence with the hydrophobic surface of the micelle cores, then the average density of surfactant molecules on the cores can be estimated. PBA-*b*-PAA 3K−12K micelles have a core radius of 7.7 nm and an aggregation number of 300. This means that there are, on average, 4500 molecules of surfactant per micelle and that the surface area per surfactant molecule on the core is around 16 Å^2. The latter value can be compared to the area per molecule of a saturated C12E6 layer at the interface between pure PBA and water at saturation. We measured this value using the Gibbs equation and interfacial tension measurements between pure PBA and C12E6 aqueous solutions (cf. Figure 10). We found an area per molecule of C12E6 at the PBA/water interface of 110 Å^2 (see Table 2). The average surface area per surfactant molecule on the micelle core of 16 Å^2 is much smaller. The hypothesis of surfactant insertion on structurally intact polymer micelles is therefore irrelevant. After addition of surfactant, there is necessarily more PBA/water interface available than in the initial state. This means that the PBA-*b*-PAA micelles, although stable to pH, ionic strength, temperature, and concentration stresses, are somehow fractionated by the addition of surfactant, which is the only way to create more core/solution interface.

The apparent cmc values of a negatively charged surfactant (SDS) in the presence of polymer were studied by use of a SDS-specific electrode. The data of Figure 2 present the potential of the electrode versus the logarithm of SDS concentration. The electromotive force (EMF) decreases linearly with log (C_{SDS}) up to the cmc, as expected from the Nernst equation. The tendency is then reversed and the potential increases with C_{SDS}. The fact that the potential is not constant above the cmc is mainly due to the fact that the ionic strength of the solution changes with the addition of SDS and hence affects the aggregation state of SDS. The cmc of pure surfactant is measured around 0.2 wt %, which is consistent with literature data at this ionic strength. In the presence of polymer, the experimental curves diverge from the Nernst equation before the cmc value of the pure surfactant system. This technique allows a clear detection of the SDS interaction with the polymer, but the data do not allow a precise determination of a critical aggregation concentration, cac. At higher concentration, a break point can be distinguished, which indicates an apparent cmc. By the same token as for C12E6, one can calculate from the apparent cmc value that there are on average 31 molecules of surfactant SDS per molecule of PBA-*b*-PAA. Again, this amount implies that the PBA-*b*-PAA micelles must fractionate upon complexation with surfactant.

3.2. Capillary Electrophoresis. Electropherograms of mixtures of d_9-PBA-*b*-PAA 3K−12K at $c = 1$ wt % and C12E6 are reported in Figure 3. For the pure polymer solution, a sharp peak is detected at an electrophoretic mobility μ_{ep} of -35×10^{-5} cm^2·V^{-1}·s^{-1}. This peak corresponds to the kinetically frozen micelles of PBA-*b*-PBA.[32] In the presence of C12E6, the electropherograms are mainly unaffected for concentrations lower and equal to 0.004 wt %. For surfactant concentrations equal to 0.02 wt % and higher, the sharp peak corresponding to the polymer micelles has disappeared. Instead, we observe a peak that becomes broader and shifts toward lower absolute values of electrophoretic mobilities with increasing surfactant concentrations. These results confirm the existence of a strong interaction between diblocks PBA-*b*-PAA and surfactant. Indeed, in the presence of 0.0225 wt % surfactant or for higher concentrations, the electrophoretic mobility decreases due to the formation of a copolymer/surfactant complex. Surfactant molecules interacting with the hydrophobic block of the copolymer act as a hydrodynamic parachute, slowing down the charged copolymer. This effect is accompanied with peak broadening since the electrophoretic mobility of the complex strongly depends on the block lengths and thus on molar mass polydispersity of each block. These results also confirm that copolymer micelles are not indestructible and that they disappear.

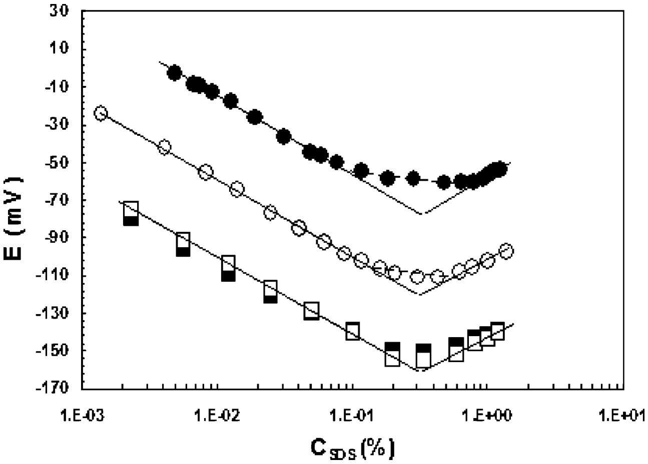

Figure 2. Potential of a SDS-specific electrode versus concentration of added surfactant SDS, in the presence of PBA-*b*-PAA 3K−12K at ionization $\alpha = 0$ and concentration (■) $C_p = 0$ wt % with a new electrode, (●) $C_p = 0.1$ wt %, (○) $C_p = 1$ wt %, and (□) $C_p = 0$ wt % with the same electrode after contact with polymer.

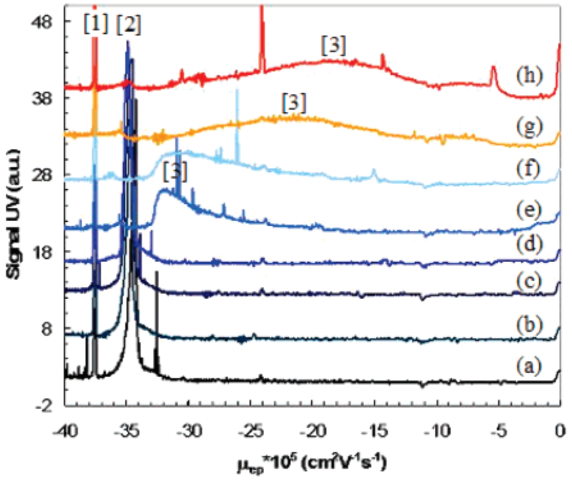

Figure 3. CE electropherograms of d_9-PBA-*b*-PAA 3K−12K with a background solution of C12E6 solutions at concentrations (a) 0, (b) 4.5×10^{-4}, (c) 2.25×10^{-3}, (d) 4.5×10^{-3}, (e) 2.25×10^{-2}, (f) 4.5×10^{-2}, (g) 2.25×10^{-1}, and (h) 4.5×10^{-1} wt %. Peak identification: 1, AA; 2, PBA-*b*-PAA; 3, PBA-*b*-PAA/C12E6 complexes.

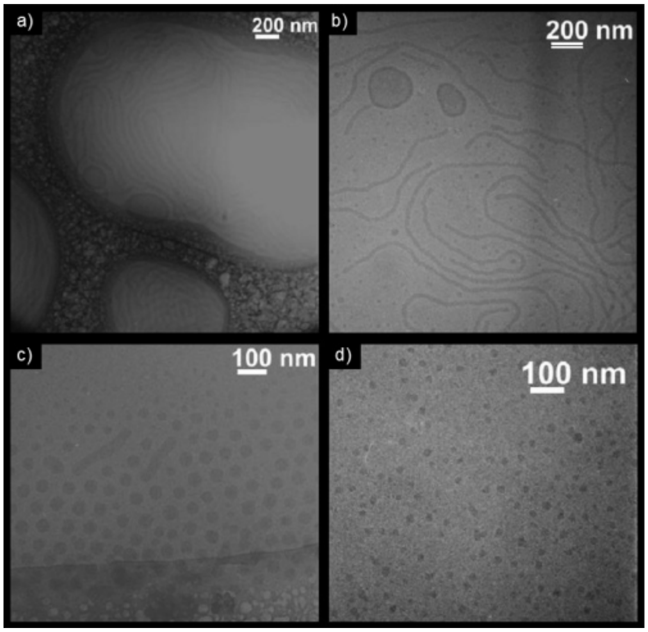

Figure 4. Cryo-TEM pictures of PBA-*b*-PAA 3K−4K solutions prepared by the cast film route at ionization $\alpha = 0$ and concentration $C_p = 2$ wt % with C12E6 surfactant added at concentrations (a) 0, (b) 0.03, (c) 0.1, and (d) 0.5 wt %.

Also, one can notice that the main effect of the surfactant is detected for surfactant concentrations that are close to the cmc value, as for surface tension measurements.

3.3. Cryo-transmission Electron Microscopy. Direct pictures of polymer−surfactant mixtures are presented in Figures 4 and 5. Figure 4a corresponds to a PBA-*b*-PAA 3K−4K solution at a concentration of 2 wt %. The solution, obtained by the "melt route", contained mainly cylindrical micelles[31] and a few vesicles. For pure polymer solutions, the visible cylinders correspond to the PBA core of the tubular micelles, whereas the coronas are not visible. The mean diameter of the PBA core is 25 nm and the length is up to micrometer size. Upon addition of surfactant (panel b), we first observe cylinders mixed with spheres. The core of the spheres have a diameter similar to the diameter of the cylinders. In the next picture (panel c), for a higher amount of added surfactant, there are mostly spheres of diameter around 30 nm and a few very short cylinders. Then, in the last picture (panel d), there are only spheres left, characterized by a large polydispersity and an average diameter of 10 nm, which is smaller than the previous spheres of 30 nm. The smallest micelles visible in the pictures have a diameter close to the value expected for a pure surfactant micelle (around 6 nm). Figure 5 shows the case of a PBA-*b*-PAA 3K−4K solution at 2 wt % prepared by the dialysis route. This solution contained monodisperse spherical polymeric micelles of diameter around 30 nm. Upon addition of surfactant SDS, the spheres become much smaller with an average size of 5 nm, which tends to say that there are mostly surfactant-like objects in solution. The same experiments have been performed with spherical micelles of 3K−12K. We observed similar trends. Since the polymer micelle cores have sizes of the same order as the surfactant micelles, the effects are less obvious.

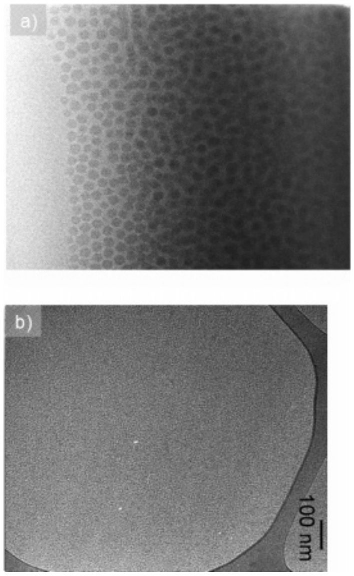

Figure 5. Cryo-TEM pictures of PBA-*b*-PAA 3K−4K solutions prepared by the dialysis route at ionization $\alpha = 0$ and concentration $C_p = 2$ wt % with SDS surfactant added at concentrations (a) 0 and (b) 8 wt %.

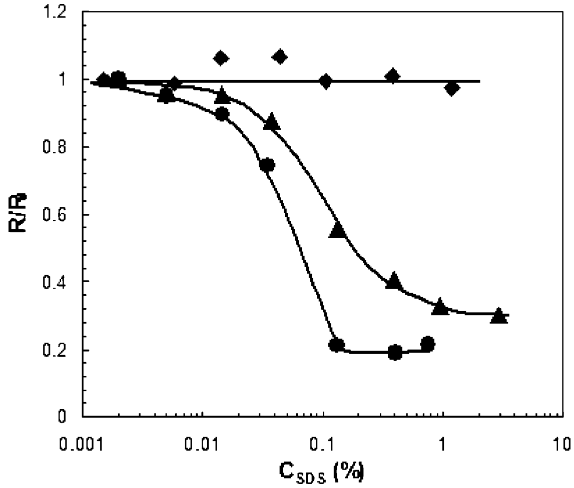

Figure 6. SLS data versus amount of added SDS for PBA-*b*-PAA solutions at ionization $\alpha = 1$ and constant polymer concentration $C_p = 0.1$ wt %: (●) PBA-*b*-PAA 1K−4K, (▲) PBA−PBA 3K−12K, and (◆) 6K−24K.

3.4. Static Light Scattering. The static light scattering (SLS) data for mixtures of PBA-*b*-PAA solutions and surfactant SDS are presented in Figure 6. The concentration of polymer is fixed in these experiments. By increasing the amount of surfactant in the mixtures, one can see that, for all polymer samples except 6K−24K, the scattered intensity decreases significantly, even though the total mass of material is increased. Since there is no effect of contrast matching in these experiments, it is clear that the objects in solution become smaller and/or fewer upon addition of surfactant. Since the scattering is mainly due to the big polymeric micelles, these data confirm again that polymer micelles have their structure strongly affected by the addition of surfactant. In the final state, that is, with an excess of surfactant, polymeric micelles are mostly disintegrated for sample 1K−4K, partially disintegrated for sample 3K−12K, and mostly not affected for the 6K−24K sample.

Figure 7 presents the same types of experimental data for the polymer PBA-*b*-PAA 3K−12K and two types of neutral surfactant, C12E6 and C6E4. Both present a scattering intensity collapse with addition of surfactant. Data for C12E6 can be directly compared to the data of interfacial tension of Figure 1. The intensity decrease stops at the C12E6 concentration corresponding to the shifted cmc. Before this point, the decrease of scattered intensity follows the decrease of interfacial tension. These data show that the disintegration of PBA-*b*-PAA 3K−12K polymer micelles occurs continuously until the shifted

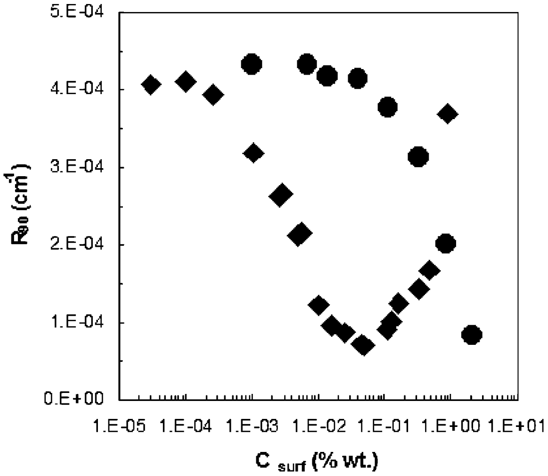

Figure 7. SLS data for PBA-*b*-PAA 3K−12K solutions at ionization α = 1 and concentration $C_p = 0.1$ wt % versus amount of added surfactant: (◆) C12E6, (●) C6E4.

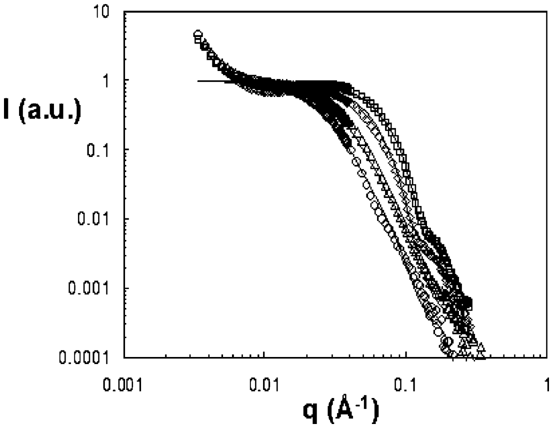

Figure 8. SANS data of PBA-*b*-PAA 3K−12K solution at 1.5 wt % and ionization α = 1 in D_2O with C12E6 at concentrations (○) 0, (△) 0.15, (◇) 0.5, and (□) 1.5 wt %.

apparent cmc value is reached. At this point, the polymer/surfactant complexation has reached saturation. Beyond this point, only additional pure surfactant micelles form. Notice that the scattering intensity increase due to pure micelles beyond the apparent cmc is more pronounced with C12E6 than with SDS or C6E4. This is simply due to the fact that C12E6 micelles are much bigger objects than SDS or C6E4 micelles and therefore scatter much more. Let us now compare the data for C12E6 and C6E4. They basically show the same trends with a decrease of the scattering intensity on the same order of magnitude for the two surfactants. However, the amount of surfactant needed to get the same effect is around 200 times larger in mass (and 300 times larger in moles) with C6E4 than with C12E6. The total amount of surfactant needed to disintegrate the polymer micelles is therefore very different from one surfactant to another. SDS is another example of this statement. Conversely, a general observation for all polymer/surfactant mixtures is that the decrease of scattered intensity starts to be significant for surfactant concentration slightly smaller than their cmc. The cmc of the surfactant seems a more relevant parameter than the relative molar amount between the polymer and the surfactant.

3.5. Small-Angle Neutron Scattering. Figure 8 presents the SANS data of PBA-*b*-PAA 3K−12K solutions at 1.5 wt % and ionization α = 1 in D_2O with C12E6 at different concentrations. Without surfactant, the intensity decreases at high *q* with a power law of −4, which means that the interface of the scattering objects is sharp. No oscillations of the form factor are visible, which means that the size distribution is rather broad. A fit by a simple polydisperse sphere model (for the PBA cores) or a core−corona model (for PBA-*b*-PAA micelles) gives an average radius for the PBA cores around 8 nm with a normalized standard deviation of $\sigma^* = \sigma/R = 0.2$. This high polydispersity in micelle sizes is common for diblock copolymer systems and is responsible for the absence of oscillation of the form factor. At high *q* and with C12E6 at 1.5 wt %, the intensity also decreases with a power law of q^{-4} and there are clear oscillations of the form factor at high *q*. The scattering intensity is also clearly shifted to higher *q* values upon addition of surfactant. Qualitatively, this means that the solution polymer/surfactant contains objects with sharp interfaces that are smaller and more monodisperse in size than solutions of pure polymer micelles. An adjustment by polydisperse spheres leads to a means radius of 3.4 nm and a normalized standard deviation of $\sigma = 0.14$. Notice that the concentration conditions of this sample correspond to the point of saturation of the complexation between the polymer and the surfactant (as determined by surface tension measurements). Since we are just at the apparent cmc of the surfactant, there are no pure-surfactant micelles in solution. Nevertheless, the SANS data indicate that the size of objects present in solution ($R \approx 3.4$ nm) is very close to the size of pure-surfactant micelles ($R \approx 3$ nm) and completely different from the size of the initial polymer micelles ($R \approx 8$ nm). At saturation, the solution of PBA-*b*-PAA 3K−12K is mostly made of surfactant-rich micelles, with size and size distribution close to pure-surfactant micelles. The disintegration of polymer micelles is therefore almost complete, which is consistent with cryo-TEM and SLS results.

In the intermediate states of disintegration, the data can be adjusted by objects of intermediate sizes, $R \approx 6.6$ nm and $\sigma \approx 0.2$ with 0.15 wt % C12E6, and $R \approx 4.2$ nm and $\sigma \approx 0.16$ with 0.5 wt % C12E6. The mechanism for disintegration seems to be a gradual decrease of the average size of a polydisperse population. The polydispersity decreases toward the total disintegration, and the size of the mixed object converges toward the state of surfactant-rich micelles with characteristics very close to those of pure-surfactant micelles.

It is also possible to take advantage of structure factor effects at low *q* to challenge the previous conclusions. The data with 0.5 and 1.5 wt % C12E6 show a faint structure peak at low *q*. The apparition of a structure peak is consistent with the fact that the scattering objects become more numerous upon addition of surfactant, so that their average distance decreases and their interaction increases. From the ratio between the absolute data and the form factor adjustment data, the positions of the structure peak are determined at 0.27 and 0.38 nm^{-1} for, respectively, 0.5 and 1.5 wt % C12E6. From these values, one can calculate the average number of PBA-PAA chains per object on the basis of the average concentration of polymer in solution. We find that the scattering objects contain on average 7.6 and 2.5 chains of PBA-*b*-PAA in the presence of, respectively, 0.5 and 1.5 wt % surfactant. Since the initial polymer micelles have an average aggregation number of 300, we confirm here that the disintegration induced by surfactant is quite complete.

4. Discussion

4.1. Poly(butyl acrylate)/Solution Interfacial Tension. In aqueous solution, PBA-*b*-PAA samples form dispersions of self-assembled aggregates that are out of equilibrium.[31] Critical micelle concentrations are extremely low, structure topologies and/or sizes of aggregates are history-dependent, and the exchange of material between objects is negligible over a time scale of several months. Irreversible behavior was shown to be a direct

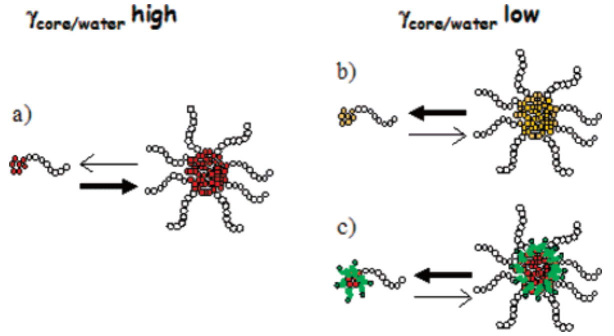

Figure 9. Schematic of the equilibrium between unimers free in solution and unimers aggregated in micelles for high (a) and low (b, c) values of interfacial tension between the core of the micelle and the solution. In case b, the chemical nature of the core is different than in case a, whereas in case c, the core is the same as in case a but surfactant is present in solution.

consequence of the high interfacial tension value between PBA and water. The cost for insertion/extraction of unimers from aggregates inhibits kinetically the exchange of unimers between micelles. External stresses, like ionic strength, temperature, and concentration, hardly affect the structure of the aggregates. Some structural reorganizations, although limited, were observed only upon charging of the PAA corona by increasing pH. These changes occurred via partial fractionation of the aggregates.

The key parameter to explain the irreversibility of the aggregation was shown to be the high value of the interfacial tension between the hydrophobic block and water. This value was measured with droplets of homopolymer PBA immersed in water and drop shape analysis. The experimental value of 20 mN/m was high enough to displace the micelle/unimer equilibrium of PBA-PAA diblock toward micelles (Figure 9a). Conversely, we have shown that this micelle/unimer equilibrium is displaced toward unimers for diblock made with a less hydrophobic first block[38] (Figure 9b). The presence of surfactant in solution is susceptible to decrease the interfacial tension between the core of the micelles and the solution and therefore to displace the equilibrium between micelles and unimers (Figure 9c). We have therefore measured the interfacial tension between a drop of homopolymer PBA and solutions of surfactants of different natures and concentration. Figure 10 shows the results for the surfactants studied, C12E6, C6E4, and SDS. The curves present classical behavior with a cmc break point. The cmc values differ for each surfactant. In all cases, the PBA−water interfacial tension at saturation decreases from an initial value of 20 mM/m down to 5 mM/m for C12E6 and C6E4 and 8 mN/m for SDS. We can now use these values to calculate the cmc of a diblock copolymer system in the presence of surfactant (i.e., versus the effective value of the core/solution interfacial tension) and the length of the hydrophobic block of the diblock. Instead of calculating the exact cmc, which implies the complex estimation of all energetic and entropic contributions from the core and the corona, we simply calculate the limit of solubility of the hydrophobic block in water.[39] We do not calculate explicitly the contribution of the PAA in the chemical potential of the unimers and the micelles. These rough assumptions are reasonable for systems with high core/water interfacial tensions values.[40] The interfacial contribution to the free energy of a PBA-*b*-PAA unimer in water and in a micelle is then written as

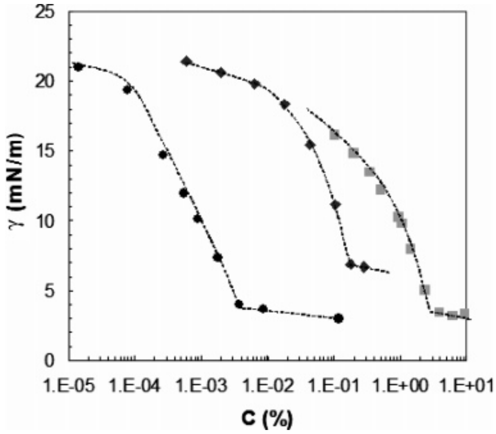

Figure 10. Interfacial tension data measured by sessile drop technique on droplets of homopolymer h-PBA immersed in surfactant solutions versus the surfactant concentration for three types of surfactant: C12E6 (●), SDS (◆), and C6E4 (■).

$$\mu_{\mathrm{unimer}}{}^{0} = \pi R_{\mathrm{uni}}{}^{2}\gamma_{\mathrm{PBA/solution}} \qquad \text{and}$$

$$\mu_{\mathrm{N}}{}^{0} = \frac{4\pi R_{\mathrm{agg}}{}^{2}\gamma_{\mathrm{PBA/solution}}}{N_{\mathrm{agg}}} \qquad (3)$$

where R_{uni} is the radius of the collapsed PBA block and Ragg is the core radius of a micelle (accessible from SANS data). R_{uni} is calculated from the mass of the PBA block and the density of PBA, with the assumption that it forms a spherical drop. The volume fraction Φ(cmc) at the cmc of the system can be approximated by the limiting solubility concentration of PBA in water, expressed by[39]

$$\phi(\mathrm{cmc}) = \exp[-(\mu_{\mathrm{unimer}}{}^{0} - \mu_{\mathrm{N}}{}^{0})/kT] \qquad (4)$$

The aggregation number being very large in our systems, the free energy of chains can be neglected (this is valid for the early stages of disintegration). Equation 4 can be transformed into

$$\mathrm{cmc} \approx \frac{100M_{\mathrm{BA}}(X_{\mathrm{BA/AA}})}{\upsilon N_{\mathrm{A}}(1 + X_{\mathrm{BA/AA}})}\exp[-\pi^{1/3}(3/4n\upsilon)^{2/3}\gamma/kT] \qquad (5)$$

where the cmc is in weight percent of sample PBA-*b*-PAA, M_{BA} is the molar mass of a monomer BA, $X_{\mathrm{BA/AA}}$ is the mass ratio of BA to AA in an idealized monodisperse diblock sample considered in this calculation, υ is the volume of a BA monomer, N_{A} is Avogadro's number, and n is the polymerization number of the PBA block. Figure 11 presents the calculated cmc values versus the mass of the first block for diblocks with $X = 0.25$, which corresponds to the series 1K−4K, 3K−12K, and 6K−24K of Figure 6. The calculations in Figure 11 are reported for two different core/water interfacial values: one of 20 mM/m, which corresponds to case of the polymer in pure water, and the other of 8 mN/m, which corresponds to the case of polymer in SDS solutions (with excess SDS to cover any core/water interface). The calculated values for the pure polymer case are very low for all PBA block masses investigated here, which is consistent with the fact that micelles are kinetically frozen. Oppositely, with the surfactant, the cmc values are greatly increased. This is consistent with our observation that the polymer micelles can disintegrate spontaneously in the presence of surfactant. More precisely, the interfacial tension argument allows us to interpret the results of Figure 7, where 160 times more

---

[38] Jacquin, M.; Futterer, T.; Muller, P.; Théodoly, O. Association of amphiphilic diblock copolymer: from colloids to macrosurfactant. Manuscript in preparation.

[39] Israelachvili, J. *Intermolecular & Surface Forces*, 2nd ed.; Academic Press: San Diego, CA, 1992; Chapt. 17.

[40] Marques, C.; Joanny, J. F.; Leibler, L. *Macromolecules* **1988**, *21*, 1051−1059.

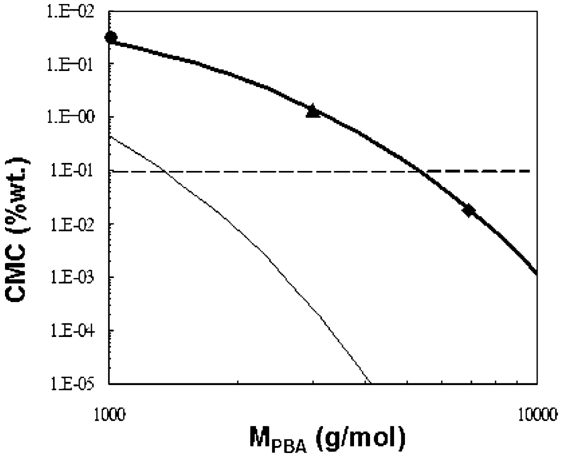

Figure 11. Calculated apparent cmc values for PBA-*b*-PAA diblocks versus the molar mass of the PBA block (thin solid line) with $\gamma_{\mathrm{PBA/solution}} = 20$ mN/m (pure water) and (−thick solid line) with $\gamma_{\mathrm{PBA/solution}} = 8$ mN/m (excess SDS in solution). The positions of PBA-*b*-PAA 1K−4K (●), PBA-*b*-PBA 3K−12K (▲), and PBA-*b*-PBA 6K−24K (◆) are indicated on the calculated curves. The dotted line shows the concentration of 0.1 wt % used in the experiment of Figure 6.

molecules of C6E4 than C12E6 are needed to achieve the disintegration of micelles. Even though enough surfactant is obviously needed to cover the core/solution interface (and allow the disintegration of all the polymer micelles), the amount of surfactant is not the only driving parameter for the micelle disintegration. A key parameter is the interfacial tension between the core of polymer micelles and the solution. Indeed, the effect of surfactants C12E6 and C6E4 on the collapse of scattered intensity in Figure 7 and the collapse of interfacial tension in Figure 10 are both shifted by almost 2 orders of magnitude. In other words, the scattered intensity (the disintegration of micelles) occurs when, and only when, the interfacial tension between the PBA cores and the solutions is sufficiently reduced.

4.2. Total or Partial Disintegration. The calculation of Figure 11 also allows us to explain why the disintegration of micelles is either total, only partial, or completely negligible. Indeed, Figure 11 shows that the cmc is strongly dependent on the molecular weight of the core block. The polymer concentration in Figure 6 was fixed at $C_p = 0.1$ wt %. From the calculation in the presence of surfactant, the calculated cmc values of PBA-*b*-PAA 1K−4K and 3K−12K are higher than 0.1 wt %, whereas the calculated cmc of PBA-*b*-PAA 6K−24K is lower than 0.1 wt %. This is consistent with the observation that micelles dissolve totally in the presence of surfactant for PBA-*b*-PAA 1K−4K and 3K−12K ($C_p <$ cmc, mostly surfactant-rich micelles in solution) and only partially for PBA-*b*-PAA 6K−24K ($C_p >$ cmc, mostly polymer-rich micelles in solution). We have seen in the Introduction that cases of total and partial disintegration have been reported in the literature and that the explanations were not consistent from one paper to the other. Zheng and Davis[24] had a complete disintegration with their diblock PB_{45}-PEO_{126} and a partial disintegration with the triblock EO_{21}-EE_{35}-EO_{21}. Their argument that triblocks are less favorable for disintegration is not really convincing. Indeed, complete disintegration is observed for triblock samples of Pluronics, whereas partial disintegration is obtained with diblock sample PB_{40}-PEO_{62} used by Nordskog et al.[25,26] In fact, all these results can be sorted by our simple criteria based on the cmc of the polymer hydrophobic core. For triblocks or diblocks, all polymer micelles with high cmc, for example, Pluronics, lead systematically to complete disintegration, whereas polymer micelles with low cmc lead to partial disintegration, for example, EO_{21}-EE_{35}-EO_{21}. EE groups are obviously more hydrophobic than PPO groups of Pluronics: interfacial tension with water of poly(ethyl ethylene) PEE is close to that of poly(propylene-*s*-ethylene), that is, 45 mN/m,[41] whereas the interfacial tension with water of poly(propylene oxide) PPO was measured at 3 mN/m with our sessile drop shape analysis experiments. For the two PB-PEO diblock samples (one studied by Zheng et al.[24] and the other studied by Norksdog et al.[25,26]), the sample with the lowest hydrophobic/hydrophilic balance, PB_{45}-PEO_{126}, and hence the highest cmc, leads to complete disintegration, whereas the sample with highest hydrophobic/hydrophilic balance, and hence the lowest cmc, leads to partial disintegration. It is difficult to go more in depth with the comparison of these literature data without the experimental determination of interfacial core/solution values with the different surfactants used. But qualitatively, the effects of efficiency of the added surfactant, hydrophobicity of the polymer, hydrophobic/hydrophilic balance of the diblock, and length of the hydrophobic block on displacement of equilibrium between large polymeric aggregates and free unimers in solution allows us to explain experimental results with our systems and the ones in the literature.

It is interesting at this point to comment on the results of Eisenberg and co-workers.[22,23] They have studied solutions of poly(styrene-*b*-acrylic acid), PS_{310}-*b*-PAA_{52}, and SDS in dioxane−water mixtures. The SDS induces a growth of the diameter of spherical aggregates and a series of morphological transitions from spheres to rods and eventually vesicles. Their observations sound a priori diametrically different from ours. However, it is important to note that their system present two main differences with ours: (i) the objects formed by their copolymers are initially at equilibrium, and (ii) the hydrophobic blocks of their diblocks are much larger than the hydrophilic blocks. The authors have been able to explain their results as follows. Due to reversibility, aggregates have complete freedom to rearrange into a new, thermodynamically stable state. Due to the very large hydrophobic block (PS_{310}-*b*-PAA_{52}), the entropic term of the hydrophobic chain in the cores is preponderant in their system over the interfacial energy term of the core. Insertion of SDS molecules on the objects' cores imposes an additional stretching of the hydrophobic blocks in the cores. The stretching results in a decrease of entropy that is compensated by structural changes of the aggregates, that is, growth of spherical micelle diameter and morphology changes from spheres to cylinders and vesicles.

For a more quantitative comparison with our system, the value of the interfacial tension of PS with the solvent used by Eisenberg and co-workers[22,23] would be helpful. However, one can remark that their solvent [a mixture of dioxane/water 88.5/11 (w/w)] was chosen to achieve reversibility of the aggregation. We know that the interfacial tension between PS and pure water is high (around 35 mN/m), so that PS-PAA aggregates are kinetically frozen in water. The presence of dioxane in their solvent is specially designed to reduce the interfacial tension between the PS and the solution. The interfacial tension term is purposely chosen to be very low whereas the entropic term is very large due to the length of the PS blocks. In conclusion, the growth of their aggregate sizes with surfactant is driven by preponderant entropic effects, whereas the decrease of our aggregate sizes is driven by preponderant interfacial energy effects.

4.3. Intermediate States of Disintegration. A gradual increase of the polymer micelles' cmc, tuned by the addition of surfactant, explains the total disintegration of polymer micelles. However,

---

(41) Lund, R.; Willner, L.; Stellbrink, J.; Radulescu, A.; Richter, D. *Macromolecules* **2004**, *37*, 9984−9993.

we have not discussed the mechanism leading from polymer micelles to disintegrated polymer micelles. Two descriptive ways have been reported in the literature: in the first way, there is always a single population of micelles whose size decreases gradually. In the second way, there is a double population of micelles, one of big polymer-rich micelles and the other of small surfactant-rich micelles, with a gradual transfer of polymer material from the former to the latter called "peeling off". From our perspective of polymer cmc tuning, the scenario with two populations makes plenty of sense, although framed differently. The two populations correspond to the two states of the complex described in Figure 9c. The big polymer-rich micelles correspond to the original polymer micelles with their core covered by surfactant. The small surfactant-rich micelles correspond to the state of polymer unimers free in solution with their hydrophobic block covered by surfactant. A gradual shift of the equilibrium constant, that is, cmc value, upon addition of surfactant results, in this view, in gradual growth of the surfactant-rich population (polymer unimers) over the polymer-rich population (polymer micelles). The polymer micelles are not peeled off but are exchanging material with the unimer population. This reasoning, based on the change of the equilibrium constant, is valid for polymeric systems that are effectively at thermodynamic equilibrium (with and without surfactant): for Pluronics systems, Cardoso da Silva et al.[20] and Jansson et al.[21] have indeed reported the detection of a double population during the disintegration phenomenon. The double-population way was also reported by Castro et al.[29,30] for another polymeric system with low (but measurable) cmc. If we now take into account a polymeric system that is completely out of equilibrium or kinetically frozen, the scenario is more difficult to reckon with. This corresponds to our system of PBA-*b*-PAA[31] and corresponds certainly to the systems of PB-PEO,[24−26] PS-PMA,[27] PtBS-PMA,[27] and PS-PEO[28] described in the literature. Indeed, PB, PS and PtBS being moieties less polar than PBA, they are expected to have a higher interfacial tension with water than PBA and must form kinetically frozen micelles in water.[31,38] It is remarkable that all these systems present strong similarities for their intermediate states of disintegration. First, the state of the solutions for these systems at small added amount of surfactant depends strongly on the way the solutions have been prepared. This history dependence is a clear proof that the intermediate states before complete disintegration of micelles are out of equilibrium or kinetically frozen. In this context, the mechanism sketched by a shift of cmc has no reason to apply to these systems. More precisely, all observations report accordingly that the intermediate states of disintegration are characterized by a population of micelles with an important polydispersity in size. This out-of-equilibrium disintegration mechanism resembles the fractionation of kinetically frozen polymeric micelles upon charging of their corona.[31] This phenomenon also leads to a population of smaller and highly polydisperse micelles by an intramicelle mechanism without implying exchange of material between micelles.

5. Conclusion

We have demonstrated the existence of a strong interaction between amphiphilic diblock copolymers PBA-*b*-PAA and small-surfactant molecules C12E6, C6E4, and SDS. This nonelectrostatic interaction changed completely the state of the polymer aqueous dispersions. Upon addition of surfactants, we observed the transition from polymer cylindrical micelles to spherical mixed micelles and from large polymer spherical micelles to small spherical surfactant-rich micelles. All the observations could be explained on the basis of evolution of the interfacial tension between polymeric micellar cores and the solutions upon addition of surfactant in solution. Interfacial tensions have been measured on droplets of pure PBA homopolymer immersed in water: the values decreased from 20 mN/m for PBA and pure water down to 5−8 mN/m for PBA and surfactant solution. This drop of surface tension controls the transition from a kinetically frozen state of polymeric micelles to a solution of mixed surfactant-rich micelles at equilibrium. This interpretation was corroborated by experiments with different surfactant types and allowed us to explain the dependencies of the transition on the concentration of each surfactant and the efficiency of the surfactant. The final value of polymer cmc also depends on the length of the hydrophobic block of the polymer so that micelles of diblocks with longest PBA blocks do not disintegrate totally. Due to the large polydispersity of the hydrophobic PBA block, the final state consists often of a partially disintegrated system. These simple thermodynamics arguments of core interfacial tension with and without surfactant permitted us to explain most observations of disintegration or no disintegration of polymer micelles with surfactant reported in the literature. The intermediate state during disintegration has also been clarified: for polymer systems at equilibrium, our approach of polymer cmc increase with addition of surfactant explained the two-population mechanism observed during disintegration. For polymer systems that form kinetically frozen objects, a most plausible path of disintegration (given that disintegration occurs during the time span of the experiment) is a fractionation of micelles. Finally, one should note that interfacial tension arguments allow us to explain all observations with diblock copolymers made of hydrophobic blocks with small molar mass. This case concerns the overwhelming majority of the systems reported in the literature. For diblock copolymers with hydrophobic blocks of large molar mass, the entropic term of the hydrophobic chain in the cores becomes important and can even be preponderant over the interfacial energy term of the core.

Acknowledgment. We thank Tarik Toulali for participation in some measurements, Lionel Porcar from NIST and Fabrice Cousin from LLB for help during the scattering runs, Marc Airiau and Annie Vacher for help with cryo-TEM experiments, and Tobias Futterer for fruitful discussions.

LA700370F